Study of the Tides around Taiwan

W. D. Liang, Y. J. Yang,
W.-S. Chuang and T. Y. Tang

Institute of Oceanography
National Taiwan University
P.O. Box 23-13
Taipei, Taiwan

Abstract

Hourly sea level data from 24 stations around Taiwan were used to analyze and assess the predictive capability of harmonic analysis. The r.m.s of sea level data at the selected stations were first calculated to study the amplitude variations. Along the west coast of Taiwan, the variation of sea level gradually increases from north and south and reaches the maximum in the neighborhood of Taichungkang. Along the east coast, the difference is small.

Using spectral analysis, the variance spectra of selected stations were examined to study the variance distribution among different frequency bands. The semi-diurnal tidal component was larger than the diurnal tidal component in the Taiwan strait and the east seas of Taiwan. In the north and south part of Taiwan, the diurnal tidal component was of the same order as the semi-diurnal component. The Luni-Solar Diurnal (K1) and Principal Solar Diurnal (O1) were the largest with K1 being slightly larger than O1. In general, the sequence of the diurnal components was largely the same in all of these stations, difference only shown in the minor components. The Principal Lunar (M2) was the largest semi-diurnal tidal component. There were larger semi-diurnal components in the north and west of Taiwan. The distribution of the semi-diurnal tidal components at Kaohsiung was more similar to that of the eastern stations of Taiwan. It also showed the notable mixed tides in the frequency band of 1/8 cph and 1/6 cph. In the low frequency band, there were remarkable annual and half-yearly variations at Keelung and Kaohsiung.

The harmonic analysis technique was also used to examine sea level data at selected stations. M2, K1, S2, O1, SA were the main constituents in these stations. K1 and M2 were the largest ones in the diurnal and semi-diurnal frequency band, respectively. In general , the result of the harmonic analysis was similar to that of the spectral analysis. In the harmonic analysis using different lengths of data, results show a decadal time scale in the variation of the tidal amplitudes and phases. A 2-year data record is optimum in the prediction of sea level using harmonic analysis. Finally, using the sea level data of the 12 selected stations in 1987, the difference of tidal phase of the main tidal constituents was studied by harmonic analysis. The semi-diurnal tide traveled from the north and south seas of the Taiwan strait and converged in the neighborhood of Taichungkang and Fanyuan. The difference of tidal phase of the semi-diurnal tide along the east coast of Taiwan was generally small. The diurnal tide traveled anti-clockwisely from the Pacific over the seas of Taiwan. It traveled southerly in the Taiwan strait and westerly in the Bashi channel. The amplitude of the semi-diurnal tide had a larger amplification factor in the Taiwan strait. . The amplification of the diurnal tide was small relatively.

The annual and interannual variations of sea level at Keelung, Kaohsiung and Fukang were calculated from the low-pass data (cut-off period is 10-day). The interannual variation exhibited the decadal and the El Niño/Southern Oscillation (ENSO) time scales.

1. Introduction

Spectral and harmonic analyses are commonly used to analyze the variations of tidal heights. In general, the power spectrum turns out to be useful in the exploration of unknown regions of the spectrum and for detection of unsuspected oscillations (Godin, 1972). Harmonic analysis is convenient in computing the amplitudes and Greenwich phase lags of the major tidal constituents. It could estimate the amplitudes and phase lags of the lower frequency of tides and would be more accurate in the prediction of tides with more data utilized in the harmonic analysis (Schureman, 1958). We will use these methods to study the tidal characteristics around Taiwan.

The location of Taiwan is just between the continental margin and the open oceans. The variations of sea level could not be only influenced by the astronomical tides, but also affected by the variations of the ocean circulation. The influences of the variations of the atmospheric characteristics could also

play an important role in the variation of sea level. Previous studies around Taiwan indicated that the variation of sea level was influenced by the intrusion of Kuroshio in the northeast (Tang and Yang, 1993; Chuang and Liang, 1994) and southwest regions (Shaw, 1989). Tang and Yang (1993) indicated that the winter intrusion of Kuroshio into the East China Sea would cause the sea level at Keelung dropped by about 40 cm. It is difficult to distinguish the variation caused by the intrusion of Kuroshio from that of the Solar Annual (SA) tidal constituents. From the variations of the adjusted sea level (removing the atmospheric pressure effect), Tang and Lin (1996) found that all the sea levels around Taiwan exhibit annual variations and more or less related to the seasonal variation of the main axis of Kuroshio.

The paper proceeds as following. Section 2 describes the distribution of stations and the correction and final quality of data. A brief review of the variations of sea level around Taiwan is also given. In Section 3, spectral analysis is applied to study the characteristics of tidal components at various frequency bands. In Section 4, harmonic analysis is applied and comparison with the results of spectral analysis is given. The spatial distribution of amplitudes and phases of major constituents and a prediction of tidal heights is also provided. Finally, discussion and summary is given in Section 5.

2. Data

Hourly sea level data from 24 stations are available from the Marine Meteorology Center (MMC) of the Central Weather Bureau (CWB) and they were used to analyze the variations of tides around Taiwan (Figure 1). The distribution of stations is rather dense along the west coast of Taiwan, but sparse in the east side. After careful examination, at least half of the available data sets are longer than 3 years and suitable for either spectral or harmonic analysis. The data measured at Keelung (1971-1996) and Kaohsiung (1969-1995) are even more complete and the results of analysis at these two stations will later be used to compare with others.

There are some spikes in the time series of the data. Some of these spikes were clearly recognized as artificial or instrumental errors. In others, it was not easy to distinguish from caused by natural phenomenon (e.g. storm surge induced by typhoon) or measurement error. The accurate recognition of spikes can depend on a well-developed storm surge model or thorough other objective analysis methods. However, as we will concentrate our attention on the astronomical arguments of tidal constituents, the spikes will be conveniently removed through subjective determination.

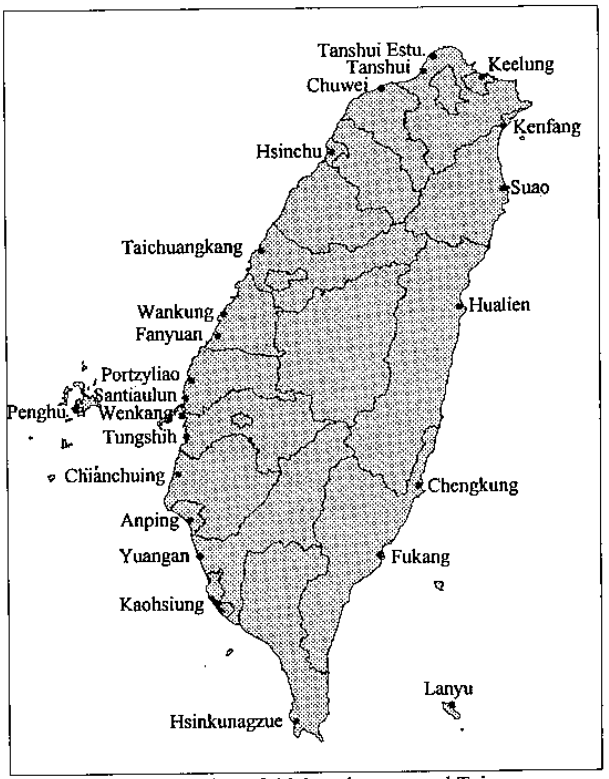

Figure 1. The distribution of tidal stations around Taiwan.

Year	1986		1987	
Station	Mean (cm)	r.m.s. (cm)	Mean (cm)	r.m.s. (cm)
Keelung	88	29	89	29
Tanshui	110	75		
Chuwei			-4	94
Taichungkang	269	134	265	134
Fanyuan	12	114	16	112
Santiaulun	30	79	28	81
Penghu	193	73	187	73
Wenkang	34	57	34	56
Chianchuing	22	41	24	41
Anping	67	30	64	30
Kaohsiung	74	26	70	27
Hsinkuangzue	9	30	11	32
Fukang	2	40	3	40
Hualien	136	39	128	40
Suao	85	39	89	38

Table 1. The r.m.s distribution of the selected tidal stations in 1986 and 1987.

In order to verify the variation of sea level around Taiwan, we choose the common period of 1986 and 1987 for comparison. Table 1 is the yearly r.m.s. distribution of some of the selected tidal stations. Along the west coast of Taiwan, the variation of sea level (after demeaning) becomes gradually high from 30 cm in the north and south parts of Taiwan to 134 cm at Taichungkang. Along the east side, the difference of the variation is small, range from 38 to 40 cm.

3. Spectral Analysis

The variance spectra of the 10 selected stations were examined to study the variance distribution among different frequency bands. They were computed using the Fast Fourier Transform (FFT) with a 10 % cosine window to reduce leakage and a convolution average method to minimize statistical errors. We show the full spectra of 4 representative stations (Keelung, Hsinchu, Kaohsiung, and Hualien at the north, west, south and east of Taiwan, respectively) in Figure 2. The semi-diurnal tidal component is larger than the diurnal component in the west and east part of Taiwan. In the north and south part, the diurnal component is of the same order as the semi-diurnal ones. In the low frequency band, the spectra of Keelung and Kaohsiung show notable annual and semi-annual variations. Low frequency energy are absent from the other two stations, which may be due to insufficient data length (1992-1995 for Hsinchu and 1985-1989 for Hualien). The semi-annual variation may be caused by the Solar Semi-Annual (SSA) effect or other non-tidal factors. As for the annual variation, it may result from many causes (e.g. the seasonal cycle of atmospheric pressure, solar heating, wind, currents etc.).

In order to closely examine the high frequency variations in Figure 2, the band of the diurnal tidal component is enlarged in Figure 3. In these stations, K1 (Luni-Solar Diurnal) and O1 (Principal Solar Diurnal) are the largest ones with K1 being slightly larger than O1. P1 (Principal Solar Diurnal) and Q1 (Larger Lunar Elliptic) are the next largest components. They are smaller than K1 and O1 by about an order of magnitude, with P1 slightly larger than Q1. In general, the sequence of the diurnal components was about the same in all of these stations, difference can only be found in the minor components. The station, Keelung, has more recognizable components than all the other stations.

The spectra of the semi-diurnal band were enlarged in Figure 4. M2 (Principal Lunar) is the largest component in this band. S2 (Principal Solar) and N2 (Larger Lunar Elliptic) are about an order of magnitude smaller and following M2. The distributions of the semi-diurnal components is quite different around Taiwan. More components show up in the north and west side of Taiwan, and extend southward along the Taiwan Strait roughly to Anping (Figure 4e). Further to the south, the semi-diurnal energy distribution of Kaoshiung is more like that of the eastern stations with less detailed structures.

Mixed tides apparently exists in the 1/8 and 1/6 cph frequency band, but their energy is much less than that of the diurnal and semi-diurnal constituents. Figure 5 and Figure 6 display the distributions of the 1/8 and 1/6 cph frequency bands separately. In the frequency band of 1/8 cph (Figure 5), the constituent of M3+NK3 is the largest one at Keelung and Hualien. In Hsinchu, MO3 and MK3 constituents are the largest ones. The components, MO3 and M3+NK3, are the same order at Kaohsiung. In the frequency band of 1/6 cph (Figure 6), the energy ratio is the same in these stations. But Keelung has more distinguishable components than the others. M4 is the largest one in this frequency band. In general, the number of mixed tides in the east and south parts of Taiwan is less than that in the west and north parts.

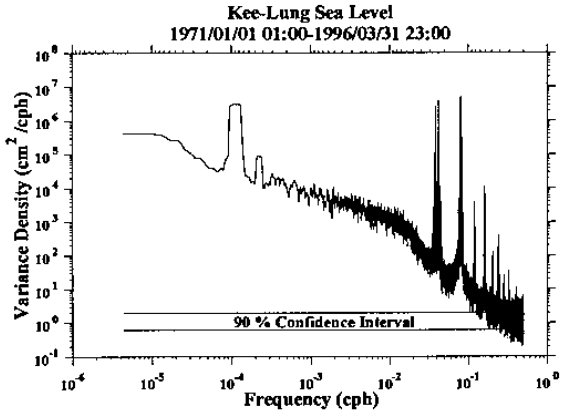

Figure 2a. The full spectrum of Keelung.
Fundamental Frequency = 4.348×10^{-6} cph.
Bandwidth=3.913×10^{-5} cph.

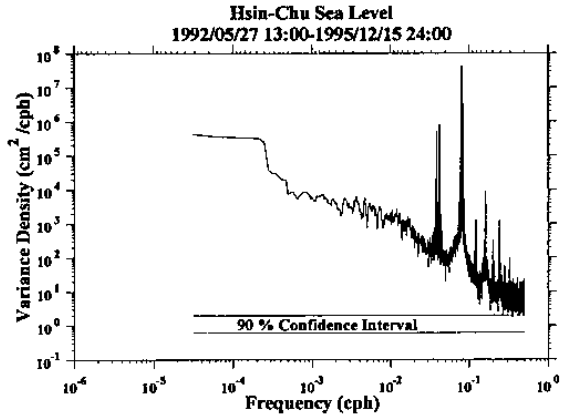

Figure 2b. The full spectrum of Hsinchu.
Fundamental Frequency = 3.125×10^{-5} cph.
Bandwidth=2.813×10^{-4} cph.

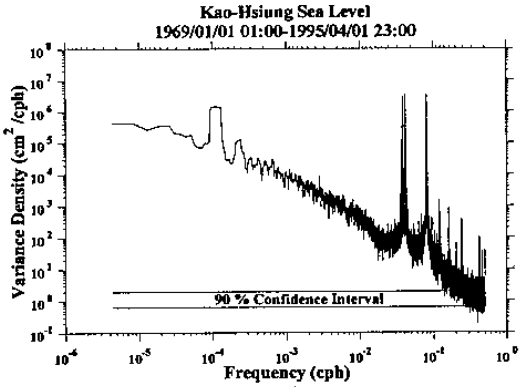

Figure 2c. The full spectrum of Kaohsiung.
Fundamental Frequency = 4.348×10^{-6} cph.
Bandwidth=3.913×10^{-5} cph.

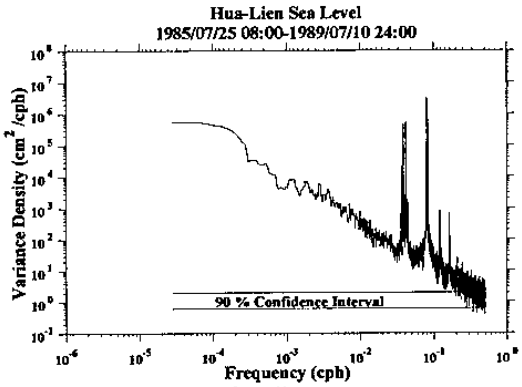

Figure 2d. The full spectrum of Hualien.
Fundamental Frequency = 2.778×10^{-5} cph.
Bandwidth=2.500×10^{-4} cph.

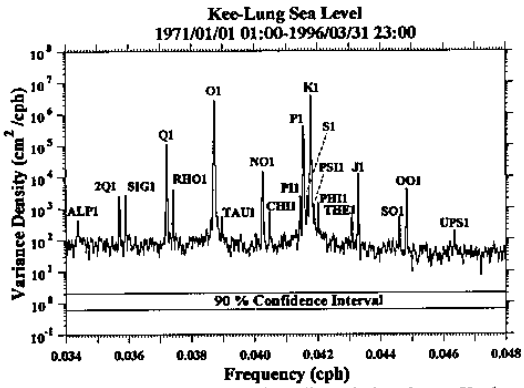

Figure 3a. The spectrum of the diurnal band at Keelung.
Fundamental Frequency = 4.348×10^{-6} cph.
Bandwidth=3.913×10^{-5} cph.

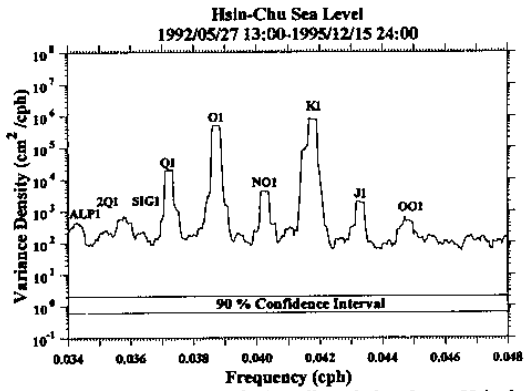

Figure 3b. The spectrum of the diurnal band at Hsinchu.
Fundamental Frequency = 3.125×10^{-5} cph.
Bandwidth=2.813×10^{-4} cph.

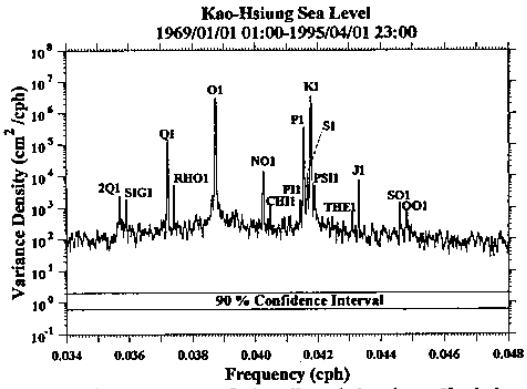

Figure 3c. The spectrum of the diurnal band at Kaohsiung.
Fundamental Frequency = 4.348×10^{-6} cph.
Bandwidth=3.913×10^{-5} cph.

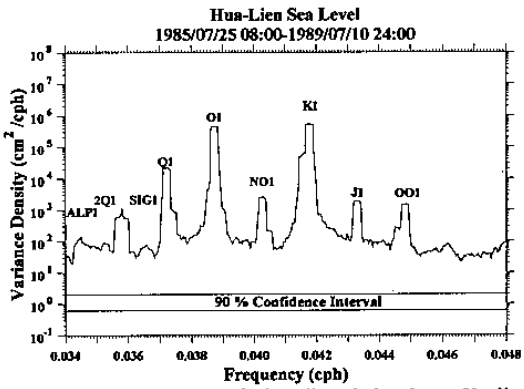

Figure 3d. The spectrum of the diurnal band at Hualien.
Fundamental Frequency = 2.778×10^{-5} cph.
Bandwidth=2.500×10^{-4} cph.

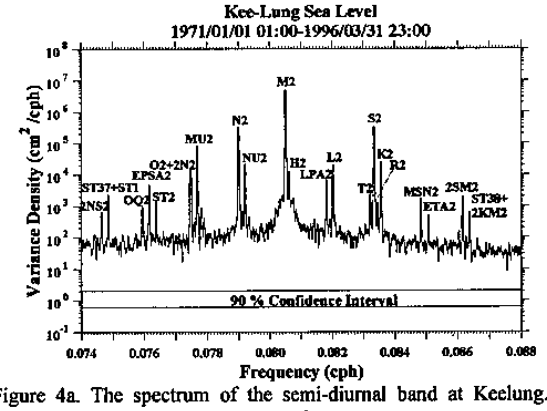

Figure 4a. The spectrum of the semi-diurnal band at Keelung.
Fundamental Frequency = 4.348×10^{-6} cph.
Bandwidth=3.913×10^{-5} cph.

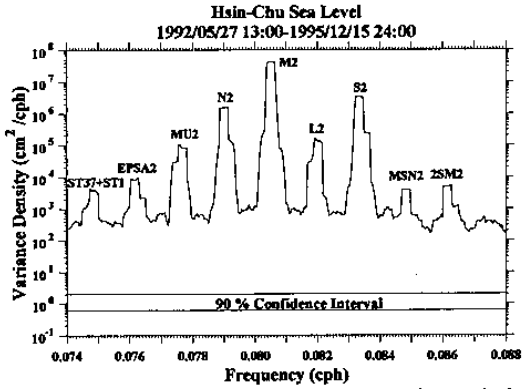

Figure 4b. The spectrum of the semi-diurnal band at Hsinchu.
Fundamental Frequency = 3.125×10^{-5} cph.
Bandwidth=2.813×10^{-4} cph.

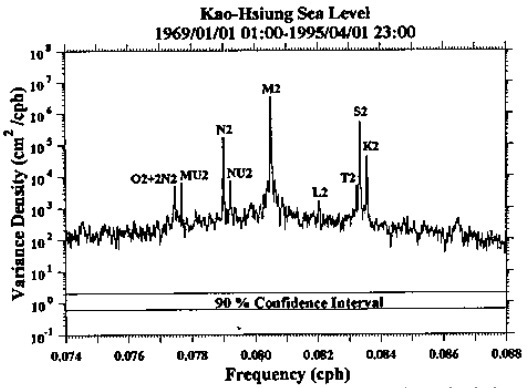

Figure 4c. The spectrum of the semi-diurnal band at Kaohsiung.
Fundamental Frequency = 4.348×10^{-6} cph.
Bandwidth=3.913×10^{-5} cph.

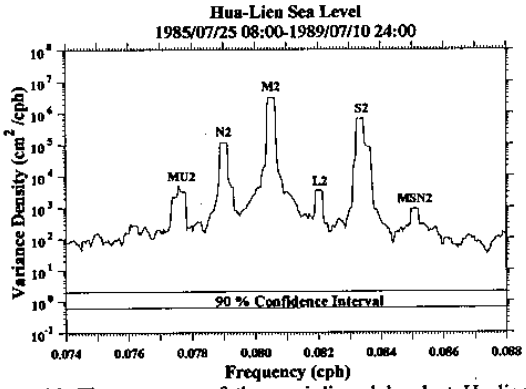

Figure 4d. The spectrum of the semi-diurnal band at Hualien.
Fundamental Frequency = 2.778×10^{-5} cph.
Bandwidth=2.500×10^{-4} cph.

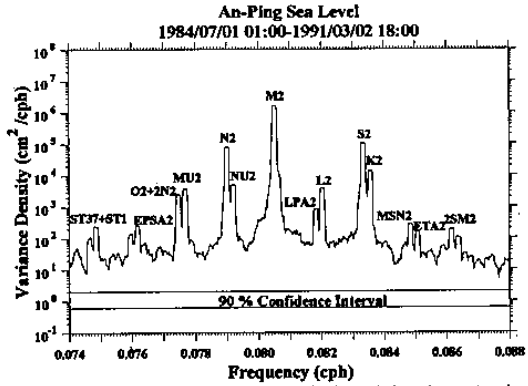

Figure 4e. The spectrum of the semi-diurnal band at Anping.
Fundamental Frequency = 1.667×10^{-5} cph.
Bandwidth=1.500×10^{-4} cph.

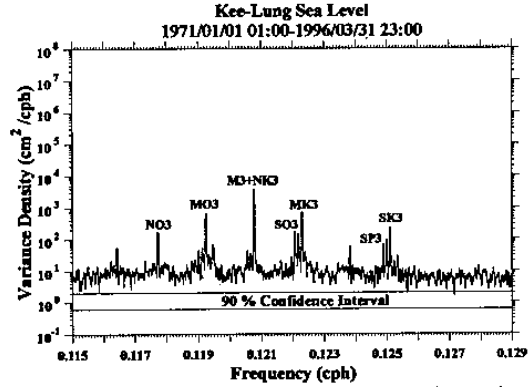

Figure 5a. The spectrum of the 1/8 cph frequency band at Keelung.
Fundamental Frequency = 4.348×10^{-6} cph.
Bandwidth=3.913×10^{-5} cph.

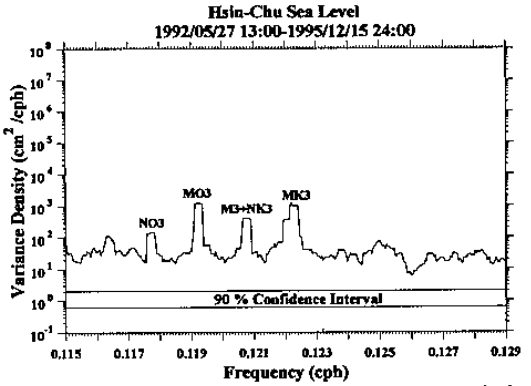

Figure 5b. The spectrum of the 1/8 cph frequency band at Hsinchu.
Fundamental Frequency = 3.125×10^{-5} cph.
Bandwidth=2.813×10^{-4} cph.

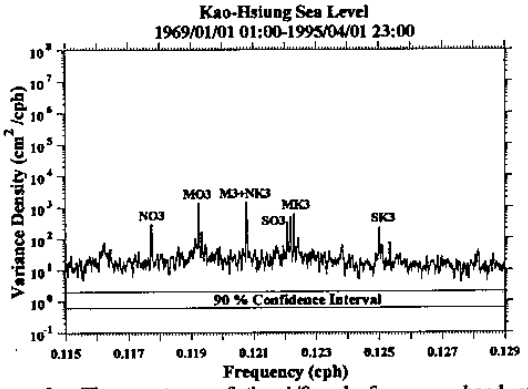

Figure 5c. The spectrum of the 1/8 cph frequency band at Kaohsiung.
Fundamental Frequency = 4.348×10^{-6} cph.
Bandwidth=3.913×10^{-5} cph.

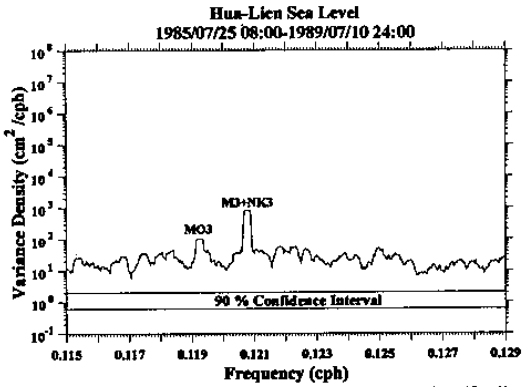

Figure 5d. The spectrum of the 1/8 cph frequency band at Hualien.
Fundamental Frequency = 2.778×10^{-5} cph.
Bandwidth=2.500×10^{-4} cph.

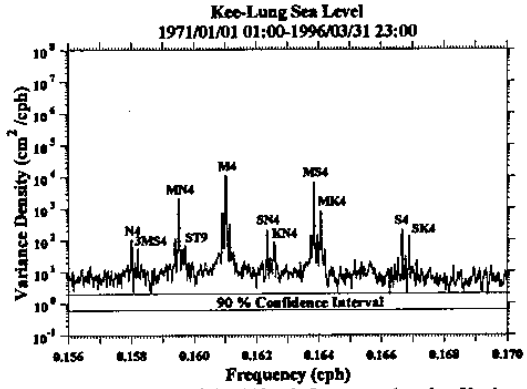

Figure 6a. The spectrum of the 1/6 cph frequency band at Keelung.
Fundamental Frequency = 4.348×10^{-6} cph.
Bandwidth=3.913×10^{-5} cph.

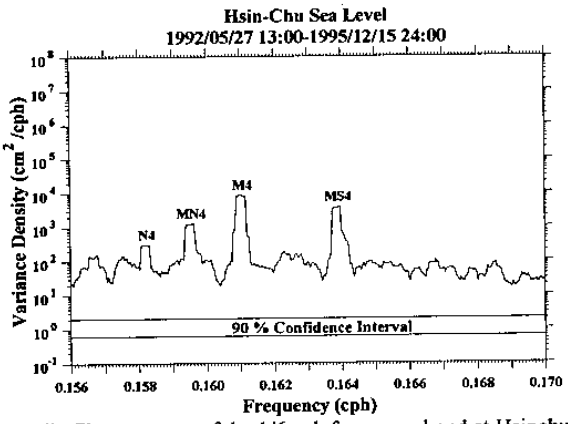

Figure 6b. The spectrum of the 1/6 cph frequency band at Hsinchu.

Fundamental Frequency = 3.125×10^{-5} cph.

Bandwidth=2.813×10^{-4} cph.

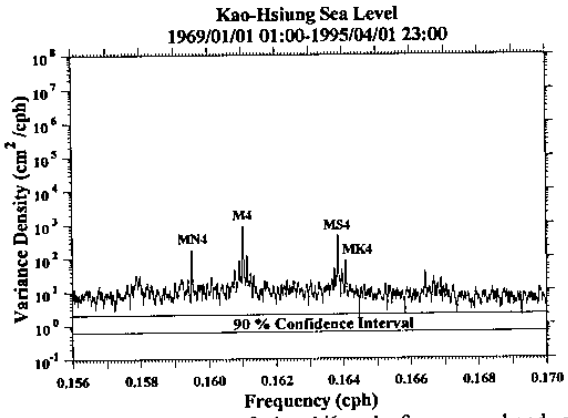

Figure 6c. The spectrum of the 1/6 cph frequency band at Kaohsiung.

Fundamental Frequency = 4.348×10^{-6} cph.

Bandwidth=3.913×10^{-5} cph.

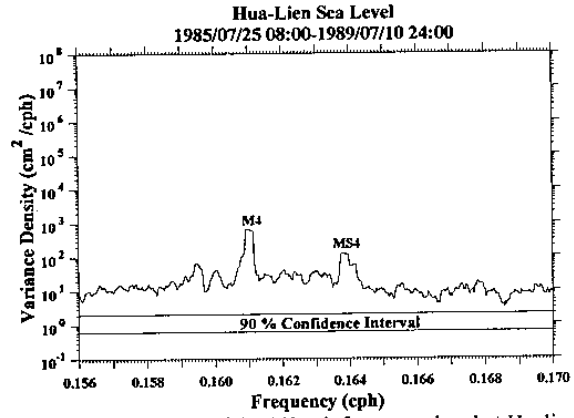

Figure 6d. The spectrum of the 1/6 cph frequency band at Hualien.

Fundamental Frequency = 2.778×10^{-5} cph.

Bandwidth=2.500×10^{-4} cph.

4. Harmonic analysis and its limitations

Harmonic analysis was also used to examine the sea level data of the selected stations. The data was the same as that used in the spectral analysis. The harmonic analysis made use of the program developed by Foreman(1987). Amplitudes and Greenwich phase lags of tidal constituents are calculated from the hourly sea level data via a least squares fit method including 69 standard components. The minimum and maximum period of standard components is 2.484 hours (M10) and 1 year (SA), respectively.

In general , the result of the harmonic analysis is similar to that of the spectral analysis. M2, K1, S2, O1, SA are the main constituents at these stations. We display the 10 largest constituents of 4 stations (Keelung, Hsinchu, Kaohsiung, and Hualien) in Table 2. The composition of the main components is basically the same and only different in sequence. Z0 is the mean of sea level. K1 and M2 are the largest ones in the diurnal and semi-diurnal frequency band, respectively. The ratio of K1 to M2 is about 1 at Kaohsiung and 0.83 at Keelung. In the west and east of Taiwan, the ratio is less than 0.5. S2 is slightly larger than K1 at Hualien. But S2 is twice as large as K1 at Hsinchu.

In order to examine the stability of the amplitude and phase analyzed from the harmonic analysis, we used different data lengths of the sea level record of 3 selected stations (Keelung, Wenkang and Kaohsiung) in the harmonic analysis. We show the results from the Keelung station in Figure 7. The amplitudes and phases of Z0, SA, P1 and S2 constituents became stable when increasing the length of the data. Nevertheless, there is a variation of decadal time scale in the amplitudes and phases of M2, K1 and O1 constituents. Ther was an abrupt change in 1976. This phenomenon also exists in the data from the other two stations.

The sea level data from 1987 were used to investigate the spatial distribution of amplitudes and phases. We show the distribution of M2 and K1 constituents in Figure 8. These are the largest components of the diurnal and semi-diurnal constituents. In Figure 8, the difference of tidal hour is referred to Greenwich. The semi-diurnal tide travels westerly from the Pacific into the northern and southern part of the Taiwan strait at the same time and then converges in the vicinity of Taichungkang and Fanyuan. The amplitude of the semi-diurnal tide increases on the way toward the central part of the Taiwan strait. The amplitude of Taichungkang is about 6-10 times larger than that of Keelung and Kaohsiung. The difference of amplitude in the east part of Taiwan is small. The diurnal tide travels anti-clockwise from the Pacific Ocean through the north part of Taiwan, and moves southerly in the Taiwan strait and later merges with another branch propagating toward the South China Sea through the Bashi Channel. The diurnal tide has a small amplification factor (15% ~ 40%) within the Taiwan Strait. These results were similar to that found by Chen and Hwung (1990).

Table 2a. The amplitude and phase of the 10 largest tidal components calculated from the harmonic analysis at Keelung.

Constitue nt	Frequency (cph)	Amplitude (m)	Phase (degree)
Z0	0.00000000	0.9054	0.00
M2	0.08051140	0.2144	276.84
K1	0.04178075	0.1779	217.12
SA	0.00011407	0.1633	203.86
O1	0.03873065	0.1439	206.60
P1	0.04155259	0.0608	223.61
N2	0.07899925	0.0543	245.67
S2	0.08333334	0.0534	280.35
Q1	0.03721850	0.0297	186.56
MU2	0.07768947	0.0266	125.23
SSA	0.00022816	0.0254	308.87

Table 2b. The amplitude and phase of the 10 largest tidal components calculated from the harmonic analysis at Hsinchu.

Constitue nt	Frequency (cph)	Amplitude (m)	Phase (degree)
Z0	0.00000000	0.0609	0.00
M2	0.08051140	1.6095	318.63
S2	0.08333334	0.4627	0.13
N2	0.07899925	0.3067	293.06
K1	0.04178075	0.2347	256.19
O1	0.03873065	0.1980	217.16
SA	0.00011407	0.1360	201.09
K2	0.08356149	0.1310	359.35
L2	0.08202355	0.0930	345.26
NU2	0.07920162	0.0787	299.26
P1	0.04155259	0.0737	250.52

Table 2c. The amplitude and phase of the 10 largest tidal components calculated from the harmonic analysis at Kaohsiung

Constitue nt	Frequency (cph)	Amplitude (m)	Phase (degree)
Z0	0.00000000	0.7496	0.00
K1	0.04178075	0.1728	276.39
M2	0.08051140	0.1721	219.66
O1	0.03873065	0.1598	254.36
SA	0.00011407	0.1086	220.31
S2	0.08333334	0.0684	233.01
P1	0.04155259	0.0559	280.89
N2	0.07899925	0.0388	206.10
Q1	0.03721850	0.0333	230.62
SSA	0.00022816	0.0251	11.23
K2	0.08356149	0.0192	221.45

Table 2d. The amplitude and phase of the 10 largest tidal components calculated from the harmonic analysis at Hualien

Constitue nt	Frequency (cph)	Amplitude (m)	Phase (degree)
Z0	0.00000000	1.3253	0.00
M2	0.08051140	0.4362	172.05
S2	0.08333334	0.1914	205.13
K1	0.04178075	0.1559	217.28
O1	0.03873065	0.1353	192.18
SA	0.00011407	0.0892	222.35
N2	0.07899925	0.0845	161.76
P1	0.04155259	0.0530	212.89
K2	0.08356149	0.0499	204.01
Q1	0.03721850	0.0293	171.78
NU2	0.07920162	0.0150	166.02

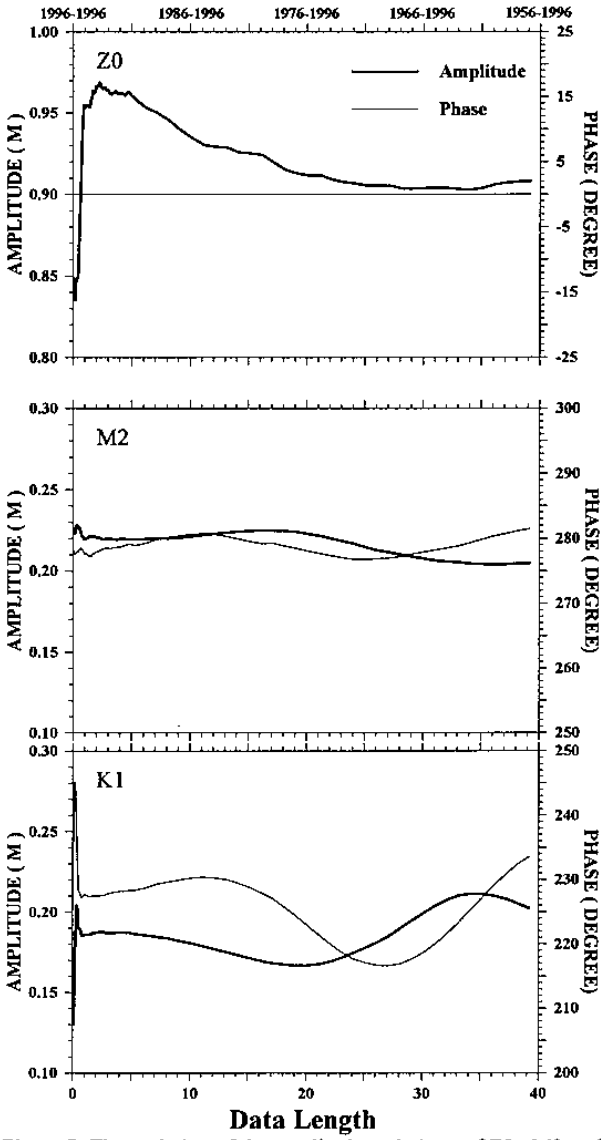

Figure 7. The variation of the amplitude and phase of Z0, M2 and K1 constituents result from the use of different data length at Keelung.

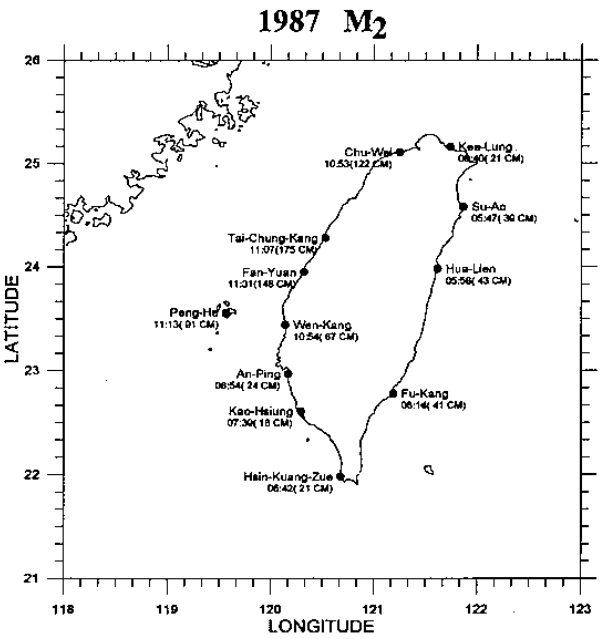

Figure 8a. The distribution of amplitudes and the differences of tidal hour of M2 (referred to Greenwich) in 1987.

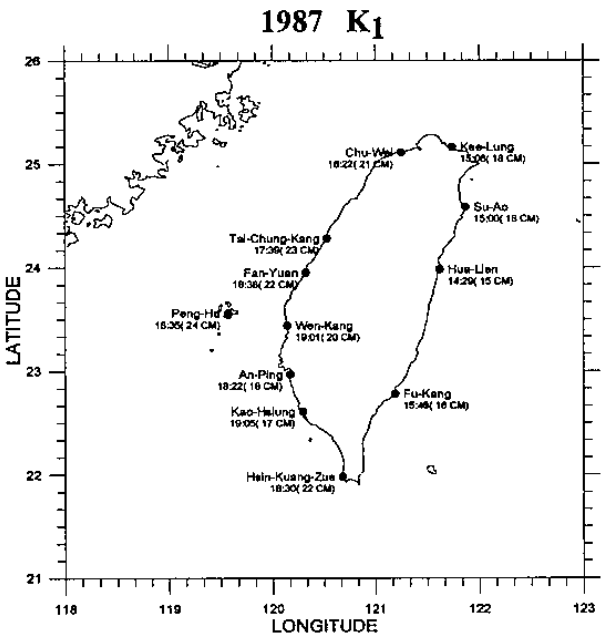

Figure 8b. The distribution of amplitudes and the differences of tidal hour of K1 (referred to Greenwich) in 1987.

From Table 2, we know that SA plays an important role in the prediction of sea level. However, as the maximum period of the components used in the harmonic analysis was only one year, the energy of low frequencies will be folded into the constituents of higher frequencies. On the other hand, increasing the length of the sea level data will not add accuracy to the predicted sea level as shown in Figure 7. Thus for practical purpose, we concluded that a sea level data length of 2 years was optimum for predicting tide in this region.

At Kaohsiung , 6 months, 12 months and 24 months' data of sea level in 1990-1991 were used to predict the sea level in 1992 by harmonic analysis. The scatter figure of observation vs. prediction was plotted in Figure 8a. The accuracy of prediction depends on the slope of the fit line. If the slope is one and the fit line crosses the origin, the predictions will be very close to the observations. The result of using 12 months' data for prediction only increases the slope from 0.827 to 0.830. When using 24 months' data to predict, the slope increases greatly to 0.953. But the scattering did not improve accordingly. Similarly, at Hsinchu, we use the 1 months, 6 months and 12 months' data of sea level from July of 1994 to June of 1995 to predict the sea level between July and October in 1995. The result of Hsinchu in Figure 8b is more accurate than that of Kaohsuing. When increasing the data length, the slope and scattering were both improved.

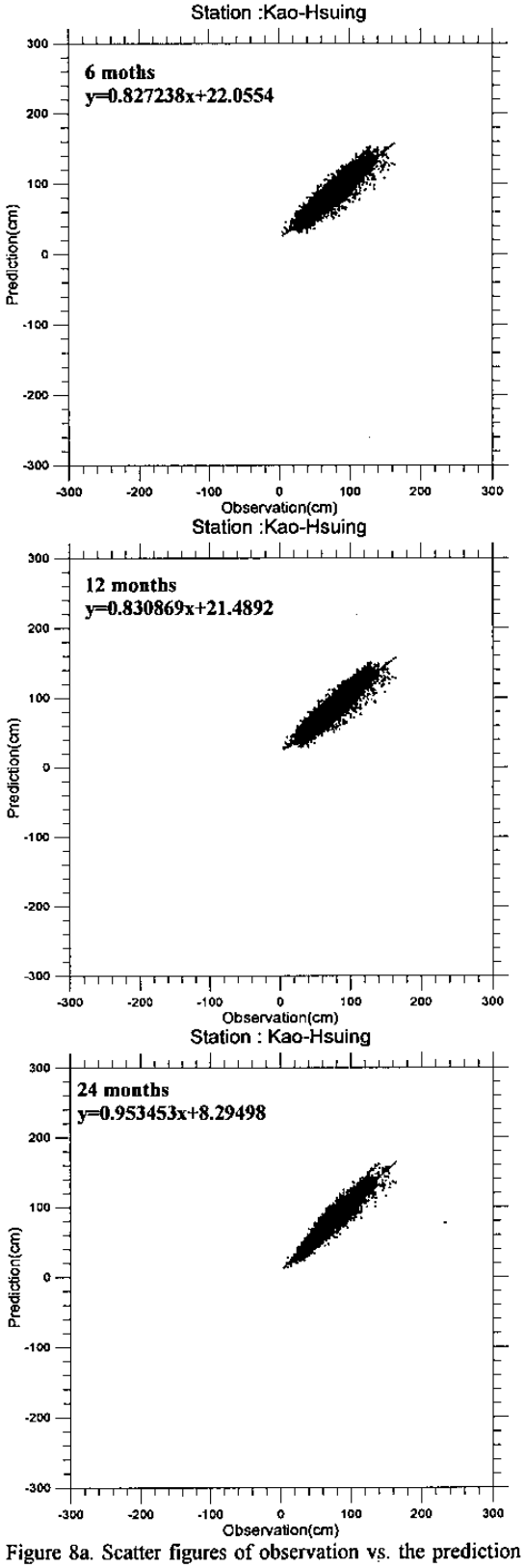

Figure 8a. Scatter figures of observation vs. the prediction results using 6 months, 12 months and 24 months' data of sea level at Kaohsiung in 1990-1991 to predict the sea level in 1992 by harmonic analysis.

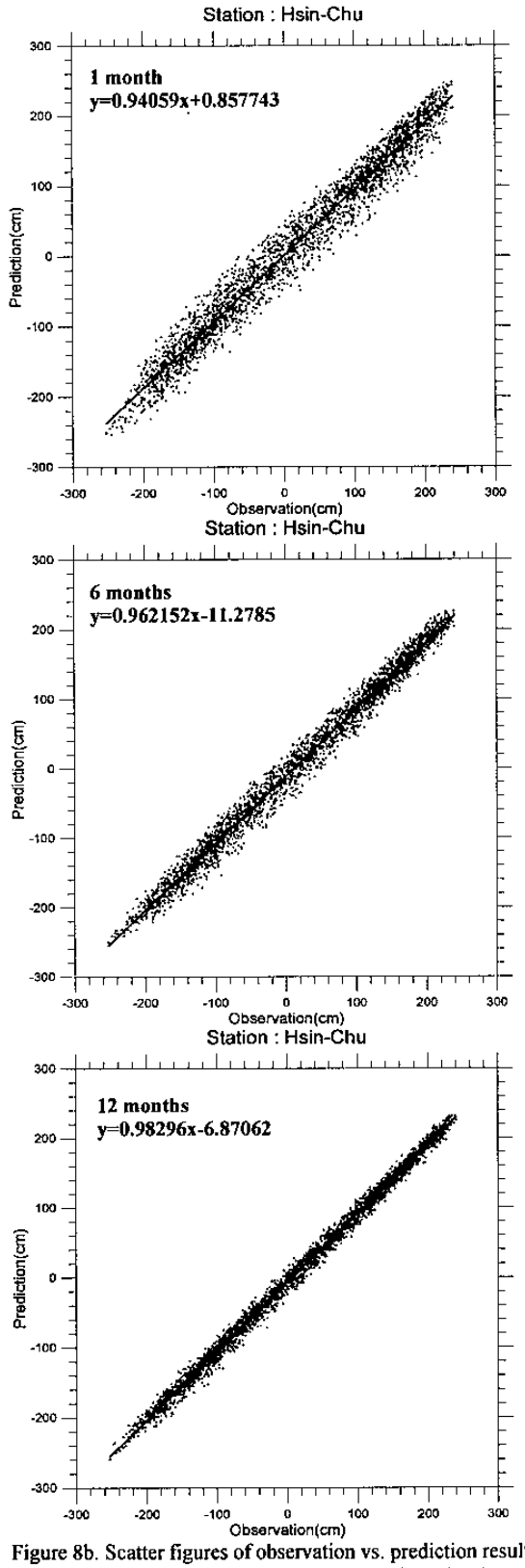

Figure 8b. Scatter figures of observation vs. prediction results using 1 months, 6 months and 12 months' data of sea level at Hsinchu from July of 1994 to June of 1995 to predict the sea level between July and October in 1995 by harmonic analysis.

5. Discussion and Summary

According to the above analysis, the variation of sea level around Taiwan not only includes the effects of the astronomical tides but also involves the influences of atmospheric and oceanic factors. For example, the seasonal variations of the atmospheric pressure and temperature, the intrusion of Kuroshio in the northeast and southwest of Taiwan, the wind field and the land and sea breezes would cause the variation of sea level which are noises for tidal signals.

At Keelung, the diurnal component is of the same order as the semi-diurnal component from the spectral and harmonic analysis. The observations of current meter moored around the region of the northeast of Taiwan by the KEEP (Kuroshio Edge Exchange Process) project indicated that the semi-diurnal tide was larger than the diurnal tide. Some of the diurnal component in Keelung may be caused by local factor (e.g. land and sea breezes). The accuracy of prediction in Kaohsiung (Figure 8a) did not increase with the data length used in the harmonic analysis. Comparing the result of Hsinchu, the tidal amplitude of Kaohsiung may be influenced by ocean circulation. The intrusion of Kuroshio could be the main cause.

The oscillations of decdal time scale in the amplitudes and phases of tidal constituents (Figure 7) motivated the following analysis. Figure 9 shows the annual and interannual variations of sea level at Keelung, Kaohsiung and Fukang. The annual variations were plotted from the low-pass data (cut-off period is 10-days) of sea level. The interannual variations were calculated from subtracting the climatological annual cycle. There are obviously seasonal variations in these stations (Figure 9a-9c). The high tide level generally begins in May, and the low tide level begins in October. Hanawa (1996) indicated that there are two distinctive patterns in an EOF analysis for SST field of the North Pacific, one is of the El Niño/Southern Oscillation (ENSO) time scale with period of 3-4 years and the other is of a decadal (DC) time scale. Data shown in Figure 9c-9d, it is similar to the SST results, the variation of decadal time scale is more obvious than that of the ENSO time scale. In 1976-1980, the anomaly of south stations (Kaohsiung and Fukang) is positive, while that of the north station (Keelung) is negative. It looks like a north-south oscillation of low latitude and mid latitude oceans (central North Pacific) (Hanawa, 1996). They all change to opposite sign in the next decade.

In summary, the results of the spectral and harmonic analysis indicate that the variations of sea level around Taiwan include the interannual, annual, diurnal, semi-diurnal and mixed tide components. The amplitude of the semi-diurnal tide has a larger amplification phenomenon in the Taiwan strait. The amplification of

the amplitude of the diurnal tide is relatively small. The diurnal components at Keelung may be caused by the land and sea breezes. The annual variation is not only induced by the astronomical tide SA, but also caused by other factors (e.g. the intrusion of Kuroshio and the seasonal variations of the atmospheric pressure and temperature). The interannual variation has ENSO time scale with period of 3-4 years and the decadal time scale. A data record of 2 years length is optimum in the prediction of sea level using harmonic analysis.

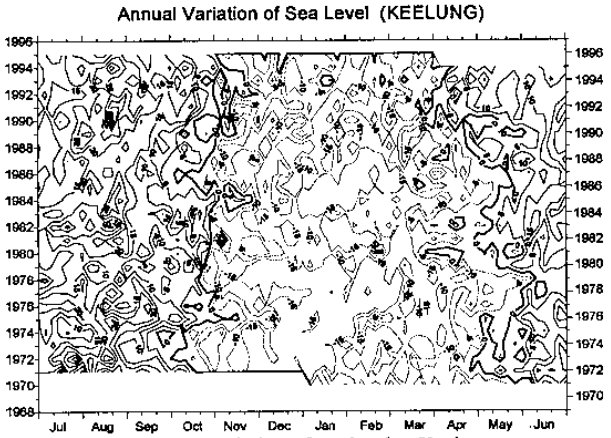

Figure 9a. The annual variation of sea level at Keelung.

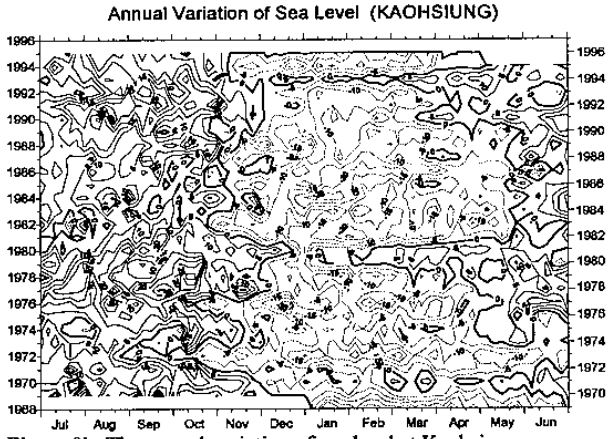

Figure 9b. The annual variation of sea level at Kaohsiung.

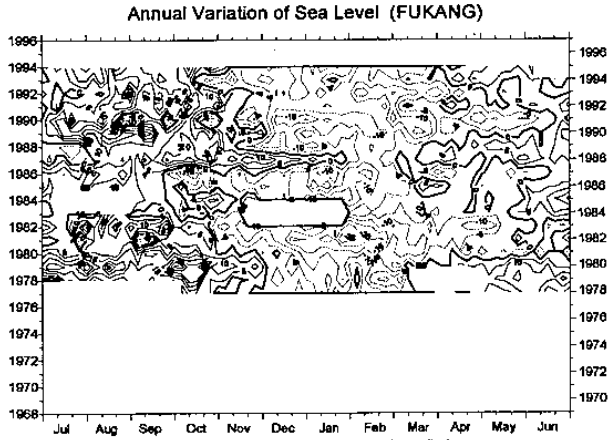

Figure 9c. The annual variation of sea level at Fukang.

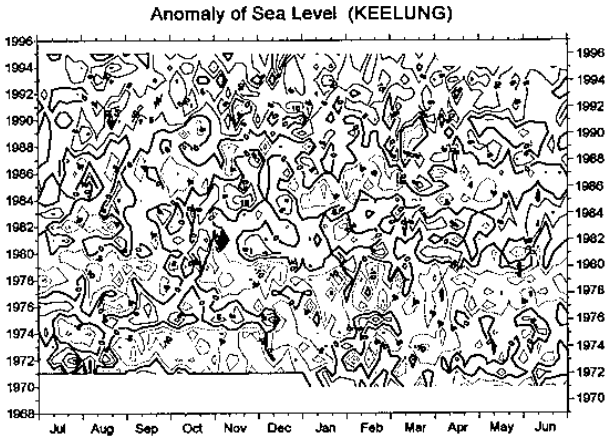

Figure 9d. The anomaly of sea level at Keelung.

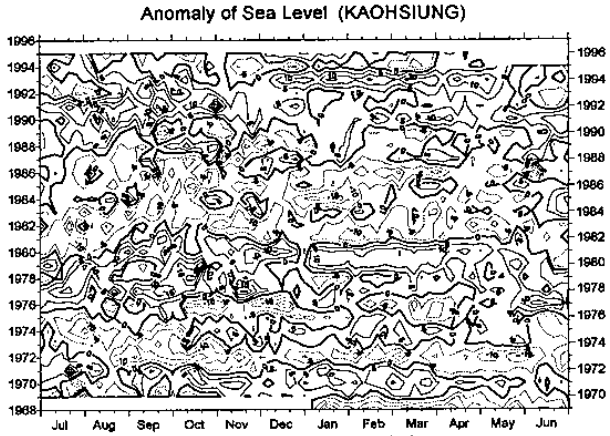

Figure 9e. The anomaly of sea level at Kaohsiung.

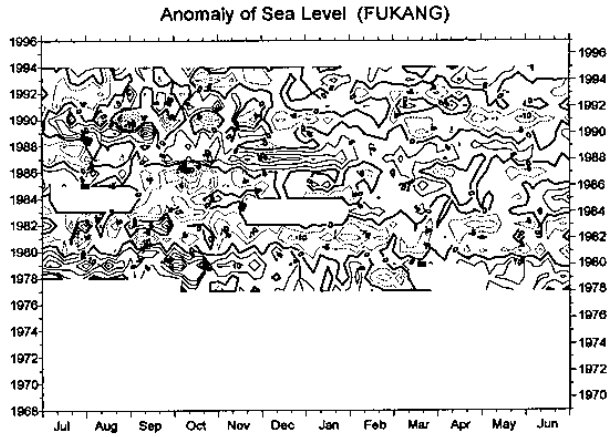

Figure 9f. The anomaly of sea level at Fukang.

Acknowledgments

This work is supported by the Central Weather Bureau under grant CWB 85-2M-08. We would like to express our cordial thanks to Mr. H. S. Hwang of the Marine Meteorology Center (MMC) of the Central Weather Bureau (CWB) for giving the suggestion and information about the sea level data.

References

Chen, Y. F. and H. H. Hwung, 1990: "Arrangements and Analysis of Tidal Records around Taiwan's

coastal Areas" , 5th Conference on Hydraulic Engineering, 1050-1063

Chuang, W.-S. and W. D. Liang, 1994: "Seasonal variability of intrusion of the Kuroshio water across the continental shelf northeast of Taiwan" , J. Oceanogr., Vol. 50, 531-542

Foreman, M. G. G., 1977: "Manual for tidal heights analysis and prediction" , Institute of Ocean Science, BC, Canada.

Hanakawa, K., 1996: "Decadal scale variability in the north Pacific" , International workshop on ocean climate variations from season to decades with special emphasis on Pacific Ocean buoy network, 30

Godin, G., 1972: The Analysis of Tides, Chapter 4, University of Tornonto Press, U.S.A. 206

Schureman, P., 1958: "Manual of harmonic analysis and prediction of tides" , U.S. Dept. of Commerce, Coast and Geodetic Survey, Special Publication No. 98.

Shaw, P.-T., 1987: "The intrusion of water masses into the sea southwest of Taiwan" , J. Geophys. Res., Vol. 94, 18,213-18,226

Tang, T. Y. and Y. J. Yang, 1993: "Low frequency current variability on the shelf break northeast of Taiwan" , J. Oceanogr., Vol. 49, 193-210